

# MOA: Efficient Scene-aware Multi-object Arrangement in VR

## Supplementary Material

Xuehuai Shi, Yuhuan Duan, Ziteng Wang, Jian Wu, Zhiwen Shao, Jieming Yin, and Lili Wang

In this document, we provide the details of the pilot user study, user studies 1 and 2 in support of the main text.

### 1 PILOT USER STUDY: COEFFICIENTS OPTIMIZATION

In this section, we conduct a pilot user study to optimize the MOA coefficients, thereby improving MOA's task performance in general multi-object arrangement scenes. MOA consists of two steps:  $MOA_s$  and  $MOA_m$ . There are three coefficients in MOA: the importance coefficient  $\alpha$  of  $MOA_s$ , the structural quantity coefficient  $\beta$ , and the element thickness coefficient  $\gamma$  of  $MOA_m$ . In the multi-object arrangement task, MOA first executes  $MOA_s$  for initial selection, then proceeds to later manipulation using  $MOA_m$ , with the efficiency of these two steps being independent of each other. Therefore, we first assess the impact of  $\alpha$  in  $MOA_s$  to find the optimal value; subsequently, we evaluate the effects of  $\beta$  and  $\gamma$  in  $MOA_m$  to determine their optimal values.

We formulate two hypotheses for the pilot user study:

**H1.** Different  $\alpha$  values used in MOA significantly affect the task performance of the initial selection step in the general multi-object arrangement scene.

**H2.** Different  $\beta$  and  $\gamma$  values used in MOA significantly affect the task performance of the later manipulation step in the general multi-object arrangement scene.

#### 1.1 User Study Design

**Apparatus.** Our system uses a PICO 4 Pro HMD powered by a workstation with a 3.8GHz Intel(R) Core(TM) i7-10700KF CPU, 32GB of RAM, an NVIDIA GeForce GTX 3080Ti graphics card, and an HTC Vive tracker. The resolution of the HMD is 2160×2160 pixels for each eye, and the field-of-view is 105°. The whole system was running at 90  $fps$  for each eye. We use the built-in programs of PICO 4 Pro to implement gaze and hand gesture tracking. Our program is developed with C# and HLSL, and is run in Unity 2021.3.8f1.

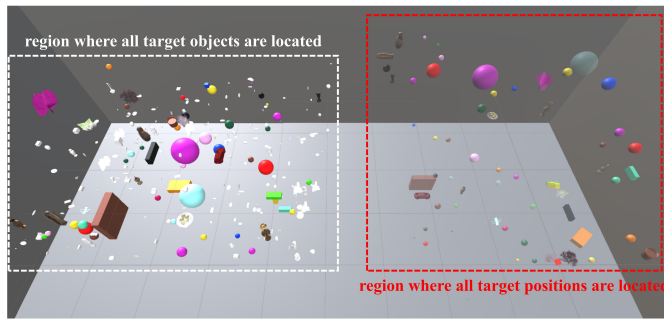


Fig. 1: Visualization of general scene.

**Test Scene Construction.** To fully simulate the complex interference and occlusion scenarios encountered during general multi-object arrangement tasks in VR, we carefully design a highly occluded general

testing scene, *general scene*, based on previous research, as shown in Fig. 1. We determine the number of objects according to the multi-object manipulation scene arrangement scheme in Maslych et al. [1], while the object shapes and target position layouts are based on findings from the multi-object arrangement review by Bergstrom et al. [2]. Following Maslych et al. [1], we set the number of candidate and target objects to the median values across all scenes, 256 and 60 respectively, and we place them randomly within the current field of view. According to Bergstrom et al. [2], 55.6% of candidate objects are spherical, 22.2% cubic, and 22.2% real-world objects, which have complex shapes such as toys and sculptures. Regarding target position layout, 40.0% are randomly distributed, 36.0% arranged in a circular layout, and 24.0% organized in a grid layout [2].

All objects and target positions in the *general scene* are fixed and static. Since the experiments in this paper aim to compare the performance and user experience across different method conditions in multi-object arrangement tasks, fixing object locations and target positions effectively eliminates distractions caused by dynamic factors and prevents non-reproducibility in experimental results. This ensures the reliability of the results when evaluating condition effects in multi-object manipulation tasks, thereby enhancing the comparability and interpretability of the data. Therefore, all test scenes in this paper have fixed object locations and target positions by design.

**Participants.** We recruit 16 participants, including nine males and seven females, aged from 18 to 50, with an average age of 27. All participants have normal vision or corrected-to-normal vision. Ten of them have experience using HMD VR applications before the study.

**Conditions.** The proposed method MOA is defined as  $MOA_s(\alpha) + MOA_m(\beta, \gamma)$ , where different coefficient values affect the multi-object arrangement task performance. Below, we give the coefficient levels.

- In initial selection,  $\alpha \in \{1/2, 2/3, 3/4, 1\}$  in  $MOA_s$  has four levels. Values of  $\alpha < 1$  mix historical and current-round importance. The value of  $\alpha$  ranges from 0 to 1. A lower  $\alpha$  emphasizes historical importance, while a higher  $\alpha$  emphasizes current-round importance.  $\alpha = 1$  condition represents using only the current round's importance, serving as a baseline where historical importance is entirely discarded.
- In later manipulation,  $\beta \in \{0, 6, 8, 10, +\infty\}$  in  $MOA_m$  has five levels, while  $\gamma \in \{3, 6, 9\}$  has three levels. The coefficient  $\beta$  defines the maximum number of guiding elements in  $\Omega$ . When  $\beta = 0$ ,  $MOA_m$  does not use  $\Omega$  to guide the later manipulation; when  $\beta = +\infty$ ,  $MOA_m$  imposes no limit on the number of elements in  $\Omega$ . The coefficient  $\gamma$  controls the thickness of all guiding elements in  $\Omega$ . The greater  $\gamma$ , the thinner the guiding elements become.

There are a total of 19 conditions in this user study, i.e.,  $MOA_s(\alpha \in \{1/2, 2/3, 3/4, 1\}) + MOA_m(\beta \in \{0, 6, 8, 10, +\infty\}, \gamma \in \{3, 6, 9\})$ .

**Task and Procedure.** This study involves two tasks: task 1 requires selecting all target objects from candidate objects using  $MOA_s$ , and task 2 involves manipulating all target objects to designated target positions using  $MOA_m$ . To maintain high engagement and retention rates for participants throughout the experiment, this study requires participants to complete the experiment over five consecutive days, ensuring that each experimental session lasts no more than 30 minutes [3]. Task 1 is completed on the first day. Before the formal experiment begins, participants spend 30 seconds using  $MOA_s(\alpha = 3/4)$  for a brief practice session. In the subsequent formal experiment, each participant needs to complete 4 trials, with each trial corresponding to one  $\alpha$  level in

$MOA_s(\alpha)$ . To balance potential learning effects, the presentation order of these four conditions is fully balanced across all 16 participants using a  $4 \times 4$  Latin Square design.

Task 2 is distributed over the second to fifth days. Before starting this task on the second day, participants spend another 30 seconds practicing with  $MOA_m(\beta = 8, \gamma = 6)$ . This task requires participants to complete all 15 trials, which correspond to all level combinations of  $\beta$  and  $\gamma$  in  $MOA_m(\beta, \gamma)$ . Considering that the number of conditions (15) makes a fully balanced design infeasible, we adopt a randomization approach: a unique trial order is generated for each participant to mitigate sequence effects and fatigue effects. Participants complete 4, 4, 4, and 3 trials respectively on the following four days, according to their individual randomized order.

For both tasks, to ensure fair comparisons, the  $x, y$  coordinates of initial positions for all conditions are fixed, the HMD is placed on the ground to ensure the participant's viewpoint height when wearing the HMD matches their actual height, and all candidate objects and target locations remain within the participants' initial field of view [2]. Each participant completes 19 trials in total. A total of 16 (participants)  $\times$  19 (conditions) = 304 trials are collected.

**Metrics.** Since the interaction mode of  $MOA_s(\alpha) + MOA_m(\beta, \gamma)$  remains consistent across different coefficient levels, the effects on task load and convenience are uniform within the same unit of interaction time. Therefore, this study evaluates only the task performance of tasks 1 and 2. We assess task performance with *selection time cost* and *manipulation time cost*. The *selection time cost* measures the time participants spend selecting all target objects during the initial selection step, while the *manipulation time cost* measures the time spent manipulating all target objects to their corresponding target positions during the later manipulation step.

## 1.2 Results and Discussion

Before analysis, data normality is checked using Shapiro-Wilk tests and Q-Q plots. Aligned Rank Transform (ART) [4] is applied to non-normally distributed data before ANOVA. We conduct ANOVA analysis for all comparisons.

Table 1 compares the *selection time cost* of participants completing task 1 using  $MOA_s(\alpha)$  with four different levels of  $\alpha$ . Since  $\alpha$  influences the weighting accumulation of the historical importance and current-round importance for  $MOA_s$ , it directly affects the judgment of  $MOA_s$  regarding potential target objects, leading to a change in the initial selection efficiency of  $MOA_s$ . Therefore, setting the appropriate  $\alpha$  enhances the task performance during the initial selection in the multi-target arrangement task. A one-way repeated measures ANOVA on *selection time cost* for the four levels of  $\alpha$  yielded a significant effect ( $F_{3,45} = 8.51, p = 1.50 \times 10^{-4}, \eta_p^2 = 0.36$ ). Therefore, H1 is supported.

The experimental results further show that when  $\alpha = 2/3$ ,  $MOA_s$  achieves the best task performance compared with the other three levels of  $\alpha$ . Therefore, we set  $\alpha = 2/3$  to achieve optimal initial selection performance in the multi-object arrangement task.

Table 2 compares the *manipulation time cost* in task 2 using  $MOA_m(\beta, \gamma)$  under different level combinations of  $\beta$  and  $\gamma$ . Since  $\beta$  and  $\gamma$  affect the visual complexity and presentation effects of  $\Omega$ . Consequently, they influence the guidance efficiency of  $\Omega$  in the later manipulation. Thus, different  $\beta$  and  $\gamma$  levels impact the *manipulation time cost* of  $MOA_m$ . To analyze these effects, a  $5 \times 3$  ( $\beta$  levels  $\times$   $\gamma$  levels) two-way repeated measures ANOVA is conducted on the *manipulation time cost* (N=16 participants, using synthetic data generated to align with means from Table 2 and readjusted standard deviations yielding moderate F-values). The analysis revealed a significant effect for

Table 2: Mean  $\pm$  SD values of *manipulation time cost* (s) using  $MOA_m(\beta, \gamma)$  with different levels of  $\beta$  and  $\gamma$ . Means are from the original design; SDs were readjusted (approx. 20% of mean) for the ANOVA results reported below.

$\beta$ Level	manipulation time cost (s)		
	$\gamma = 3$ (Thick)	$\gamma = 6$ (Medium)	$\gamma = 9$ (Thin)
$\beta = 0$	524.8 $\pm$ 105.0	526.6 $\pm$ 105.3	522.8 $\pm$ 104.6
$\beta = 6$	458.2 $\pm$ 91.6	445.4 $\pm$ 89.1	496.9 $\pm$ 99.4
$\beta = 8$	445.4 $\pm$ 89.1	<b>415.5 <math>\pm</math> 83.1</b>	478.1 $\pm$ 95.6
$\beta = 10$	483.7 $\pm$ 96.7	438.6 $\pm$ 87.7	464.3 $\pm$ 92.9
$\beta = +\infty$	508.6 $\pm$ 101.7	487.4 $\pm$ 97.5	473.0 $\pm$ 94.6

$\beta$  ( $F_{4,60} = 23.12, p = 1.35 \times 10^{-11}, \eta_p^2 = 0.61$ ), a significant effect for  $\gamma$  ( $F_{2,30} = 3.59, p = 4.01 \times 10^{-2}, \eta_p^2 = 0.19$ ), and a significant interaction effect between  $\beta$  and  $\gamma$  ( $F_{8,120} = 4.89, p = 3.06 \times 10^{-5}, \eta_p^2 = 0.25$ ). The significant interaction indicates that the effect of  $\beta$  on *manipulation time cost* depends on the level of  $\gamma$ , and vice versa. Given these significant effects, H2 is supported.

Experimental results suggest that when  $\beta = 8$  and  $\gamma = 6$ ,  $MOA_m$  achieves the best task performance (415.5s). This represents an approximate  $1.3 \times$  speedup compared with when the  $\Omega$  guidance was disabled ( $\beta = 0$ ). While specific post-hoc comparisons would typically be performed on original experimental data to detail pairwise differences, the ANOVA results confirm the interactive influence of these coefficients.

In conclusion,  $MOA_s(\alpha = 2/3) + MOA_m(\beta = 8, \gamma = 6)$  is regarded as the optimal condition in performing multi-object arrangement tasks, as it achieves the best task performance compared with the other tested conditions in this pilot study. Therefore, in all subsequent user studies, we set  $MOA$  to  $MOA_s(\alpha = 2/3) + MOA_m(\beta = 8, \gamma = 6)$ .

## 2 USER STUDY 1: INITIAL SELECTION EVALUATION

After obtaining the optimized coefficients of MOA, we conduct user study 1 to quantify the task performance and user experience of MOA's initial selection ( $MOA_s$ ) in the multi-object arrangement task. Since existing multi-object initial selection methods include both controller-based and controller-free approaches, we evaluate  $MOA_s$  by comparing it with state-of-the-art methods from both controller-based and controller-free categories. We formulate a hypothesis for user study 1: H3. Compared to state-of-the-art controller-free and controller-based multi-object initial selection methods,  $MOA_s$  achieves significant improvements in task performance, task load, and convenience during the initial selection step of the general multi-object arrangement task.

### 2.1 User Study Design

**Participants and Apparatus.** We recruit 16 participants, ten males and six females aged between 19 and 31, with normal vision or corrected-to-normal vision. Ten have experience in using HMD VR applications, and none report balance disorders. None of them are in the pilot user study. The apparatus used in this user study is the same as in the pilot user study.

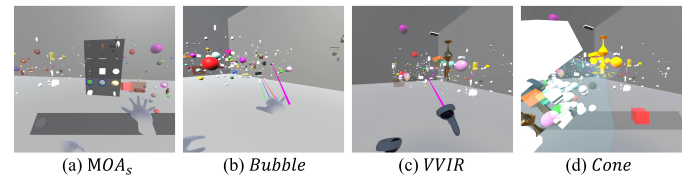


Fig. 2: Visualization of performing initial selection in *general scene* by using (a) the proposed  $MOA_s$ , (b) *Bubble*, (c) *VVIR*, and (d) *Cone* in *general scene*.

**Condition.** To comprehensively demonstrate the effectiveness of the proposed  $MOA_s$ , we compare it not only with the state-of-the-art controller-free multi-object initial selection method *Bubble* [5], but

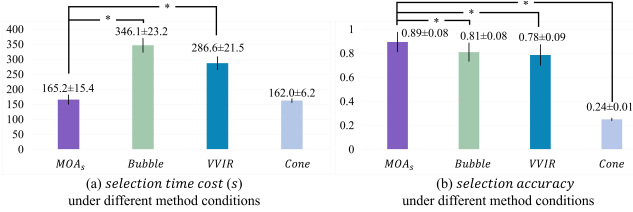


Fig. 3: Mean and standard deviation of (a) *selection time cost* and (b) *selection accuracy* in the initial selection using *MOAs*, *Bubble*, *VVIR*, and *Cone*. Asterisks indicate significant differences.

also with the state-of-the-art controller-based methods *VVIR* [6] and *Cone* [1]. Therefore, the method conditions in User Study 1 include *MOAs*, *Bubble*, *VVIR*, and *Cone*, as shown in Fig. 2.

**Task and Procedure.** The task requires participants to use all method conditions to select all target objects in *general scene*. Before starting, participants use *MOAs*, *Bubble*, *VVIR*, and *Cone* to select three specified target objects from 256 candidate objects in the *general scene*, spending an average of 30 seconds on each method condition. To ensure fair comparisons, the initial positions for all conditions are set the same as those in the pilot user study. Each participant completes 4 trials. To counteract learning and fatigue effects, the presentation order of the four method conditions is counterbalanced across participants using a balanced  $4 \times 4$  Latin Square design. After each trial, participants complete the NASA-TLX and SUS questionnaires. Completing all trials takes an average of 16 minutes per participant. A total of 16 (participants)  $\times$  4 (method conditions) = 64 trials are collected.

**Metrics.** We use the objective metrics *selection time cost* and *selection accuracy* to quantify the task performance of the initial selection step in the multi-object arrangement task. The *selection time cost* is defined in the metrics of Section 1.1. The *selection accuracy* refers to the ratio of the number of target objects selected by the participants to the total number of objects selected. To evaluate task load, we use the standard NASA-TLX questionnaire [7]. To evaluate convenience, we use the System Usability Scale (SUS) [8] for each method condition.

## 2.2 Results and Discussion

We examine the normal distribution of the data using Shapiro-Wilk tests and Q-Q plots before analysis, and utilize the ART to perform transformations for non-normally distributed data. Then, we conduct ANOVA analyses for all comparisons, reporting effect sizes wherever feasible. Additionally, we perform Bonferroni post-hoc analyses to examine individual differences between *MOAs* and (*Bubble*, *VVIR*, *Cone*).

Table 3: Post-hoc analysis of between *MOAs* and other conditions for task performance metrics in user study 1 using Bonferroni.

metric	comparison	mean dif.	std. dif.	p-value
selection time cost	<i>MOAs</i> vs <i>Bubble</i>	-178.8	6.2	$6.0 \times 10^{-36}$
	<i>MOAs</i> vs <i>VVIR</i>	-119.4	6.2	$1.9 \times 10^{-26}$
	<i>MOAs</i> vs <i>Cone</i>	5.3	6.2	1.0
selection accuracy	<i>MOAs</i> vs <i>Bubble</i>	0.8	0.0	$7.0 \times 10^{-3}$
	<i>MOAs</i> vs <i>VVIR</i>	0.1	0.0	$3.0 \times 10^{-4}$
	<i>MOAs</i> vs <i>Cone</i>	0.2	0.0	$1.6 \times 10^{-23}$

**Task Performance.** Regarding task performance, Fig. 3 visualizes the comparisons of *selection time cost* and *selection accuracy* during the initial selection step of the multi-object arrangement task in *general scene* under four different conditions. The effect test across the four conditions for *selection time cost* yields ( $F_{3,45} = 425.45$ ,  $p = 2.26 \times 10^{-40}$ ,  $\eta_p^2 = 0.95$ ), and for *selection accuracy* yields ( $F_{3,45} = 279.79$ ,  $p = 3.22 \times 10^{-35}$ ,  $\eta_p^2 = 0.93$ ), indicating significant differences among the conditions in task performance. Table 3 shows the post-hoc statistical results comparing *MOAs* with the other three

conditions for both *selection time cost* and *selection accuracy*, using the Bonferroni method. *MOAs* quickly extracts potential target objects in highly occluded scenes due to its object importance-driven selection mechanism and reduces interference and uncertainty during the initial selection step thanks to an efficient interaction mode that enables simultaneous selection. Compared with *Bubble* and *VVIR*, *MOAs* achieves significant improvements in both *selection time cost* and *selection accuracy*, demonstrating clear advantages in task performance over these conditions.

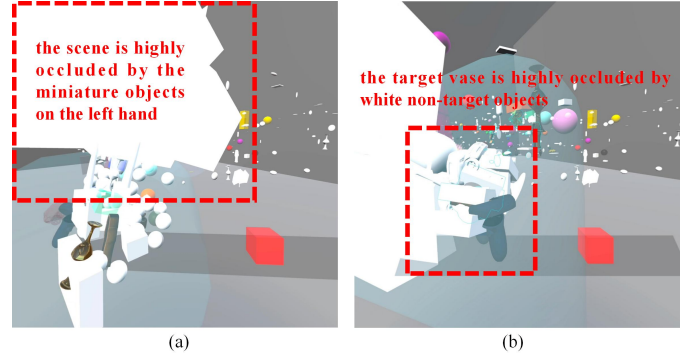


Fig. 4: Visualization of performing initial selection using *Cone* in *general scene*.

Table 4: Statistical results of scores (mean value  $\pm$  standard deviation) in NASA-TLX questionnaire under different conditions in user study 1.

QID	Mean $\pm$ SD NASA-TLX scores			
	<i>MOAs</i>	<i>Bubble</i>	<i>VVIR</i>	<i>Cone</i>
Q1	28.1 $\pm$ 5.7	30.6 $\pm$ 6.6	28.9 $\pm$ 8.5	43.8 $\pm$ 8.9
Q2	58.1 $\pm$ 12.4	60.3 $\pm$ 11.0	58.1 $\pm$ 12.4	57.5 $\pm$ 11.8
Q3	58.8 $\pm$ 5.0	70.0 $\pm$ 10.7	68.1 $\pm$ 9.8	63.1 $\pm$ 7.7
Q4	30.3 $\pm$ 7.4	47.5 $\pm$ 4.8	35.6 $\pm$ 5.4	55.6 $\pm$ 11.8
Q5	48.1 $\pm$ 11.7	54.7 $\pm$ 7.6	52.5 $\pm$ 8.4	58.4 $\pm$ 8.1
Q6	32.2 $\pm$ 11.8	47.2 $\pm$ 10.0	53.1 $\pm$ 11.2	62.2 $\pm$ 10.6
TOTAL	42.6 $\pm$ 6.1	51.7 $\pm$ 4.3	49.1 $\pm$ 4.3	56.7 $\pm$ 3.6

Fig. 4 illustrates the initial selection process using *Cone* in a *general scene*. The scale of the selectable region is set by the default farthest function [1]. Due to the dense distribution of objects in the *general scene* and the wide variation in object sizes, target objects are often heavily occluded by non-target objects (marked in white) within the minimal 3D capsule for selection, as shown in Fig. 4 (a). When a participant attempts to select the target vase within this minimal capsule using the controller, the extensive overlap causes multiple non-target objects to be selected alongside the target vase, resulting in a high number of erroneous selections, as depicted in Fig. 4 (b). As a result, although the *selection time cost* for *Cone* does not differ significantly from that of *MOAs*, the *selection accuracy* of *Cone* is  $3.7 \times$  lower than that of *MOAs*. With a selection accuracy below 30%, *Cone* produces excessive invalid selections, limiting its effective application. Therefore, *MOAs* demonstrates a significant advantage over *Cone* in terms of task performance. Thus, we obtain **Conclusion 1**: *MOAs* significantly improves the task performance with all state-of-the-art controller-free and controller-based multi-object selection methods in the initial selection step of the multi-object arrangement task in *general scene*.

**Task Load.** Regarding task load, Table 4 details the NASA-TLX questionnaire scores under different conditions. The effect test across the four conditions for the NASA-TLX total score yields ( $F_{3,45} = 25.77$ ,  $p = 7.76 \times 10^{-11}$ ,  $\eta_p^2 = 0.58$ ), indicating significant differences in task load among conditions.

Table 5 presents the post-hoc statistical results comparing *MOAs* with the other three conditions for the NASA-TLX score. Based on participants' report, although *MOAs* requires the additional activation

Table 5: Post-hoc analysis of between  $MOA_s$  and other conditions for the NASA-TLX total score in user study 1 using Bonferroni.

metric	comparison	mean dif.	std. dif.	p-value
Q1	$MOA_s$	<i>Bubble</i>	-2.5	$9.6 \times 10^{-1}$
		<i>VVIR</i>	-0.8	1.0
		<i>Cone</i>	-15.7	$7.5 \times 10^{-16}$
Q2	$MOA_s$	<i>Bubble</i>	-2.2	1.0
		<i>VVIR</i>	0.0	1.0
		<i>Cone</i>	0.6	1.0
Q3	$MOA_s$	<i>Bubble</i>	-11.2	$3.0 \times 10^{-2}$
		<i>VVIR</i>	-9.3	$1.8 \times 10^{-2}$
		<i>Cone</i>	-4.3	$9.3 \times 10^{-1}$
Q4	$MOA_s$	<i>Bubble</i>	-17.2	$3.7 \times 10^{-7}$
		<i>VVIR</i>	-5.3	$3.7 \times 10^{-1}$
		<i>Cone</i>	-25.3	$4.0 \times 10^{-12}$
Q5	$MOA_s$	<i>Bubble</i>	-6.6	$2.7 \times 10^{-1}$
		<i>VVIR</i>	-4.4	$9.3 \times 10^{-1}$
		<i>Cone</i>	-10.3	$1.3 \times 10^{-2}$
Q6	$MOA_s$	<i>Bubble</i>	-15.0	$3.4 \times 10^{-4}$
		<i>VVIR</i>	-20.9	$6.0 \times 10^{-7}$
		<i>Cone</i>	-30.0	$2.1 \times 10^{-11}$
TOTAL	$MOA_s$	<i>Bubble</i>	-9.1	$4.0 \times 10^{-6}$
		<i>VVIR</i>	-6.5	$1.0 \times 10^{-2}$
		<i>Cone</i>	-14.1	$2.5 \times 10^{-11}$

of the candidate panel to conveniently select objects, partially offsetting its advantage in physical demands, its score in Q2 (physical demands) is comparable to that of the state-of-the-art controller-free and controller-based methods. Although *Bubble* supports parallel multi-object selection, its reliance on simultaneous multi-finger pointing interactions makes it highly prone to selection errors in target-dense and occluded scenes.  $MOA_s$  effectively circumvents selection difficulties in highly occluded environments by efficiently rearranging target objects onto a candidate panel. Despite the initial step of generating the panel,  $MOA_s$  performs comparably to *Bubble* in terms of mental demand (Q1) and physical demand (Q5). However,  $MOA_s$  eliminates the repeated attempts and error corrections caused by occlusion, leading to significant advantages in terms of time pressure (Q3), self-perceived performance (Q4), and frustration (Q6). Ultimately, these advantages collectively contribute to  $MOA_s$  significantly outperforming *Bubble* in NASA-TLX total score.

In comparison to the controller-based method condition *VVIR*, according to participants' feedback, *VVIR* exhibits high efficiency in selecting a small number of multiple targets due to its ability to select targets with small controller movements. This precision of single-point operation allows  $MOA_s$  to perform comparably to *VVIR* in terms of mental demand (Q1), self-perceived performance (Q4), and physical demand (Q5). However, when the task extends to a large number of multiple targets, *VVIR* requires participants to make repeated and fine-grained aiming adjustments to select them one by one. In contrast,  $MOA_s$ ' parallel selection mode allows participants to naturally and efficiently confirm multiple targets at once, resulting in overwhelmingly significant advantages in terms of time pressure (Q3) and frustration (Q6). Consequently, this makes  $MOA_s$  significantly better than *VVIR* in NASA-TLX total score.

In comparison to another controller-based method condition *Cone*, *Cone* employs a strategy of "broadly selecting with a cylinder first, and then finely picking from within." This macro-capture mechanism provides time efficiency when dealing with spatially concentrated target groups, thus  $MOA_s$  performs comparably to *Cone* in terms of time pressure (Q3). However,  $MOA_s$  allows participants to directly and precisely click on targets in the generated panel, avoiding the cumbersome two-step operation of "coarse selection followed by fine selection"

inherent in *Cone*. This fundamental simplification of the interaction flow greatly reduces the participant's cognitive load and operational uncertainty, resulting in significant advantages for  $MOA_s$  in terms of mental demand (Q1), self-perceived performance (Q4), physical demand (Q5), and frustration (Q6). Ultimately, these comprehensive experience improvements make  $MOA_s$  significantly better than *Cone* in NASA-TLX total score.

The p-values indicate that  $MOA_s$  achieves a significantly lower NASA-TLX total score than all other conditions. Therefore, we conclude **Conclusion 2**: Compared with all state-of-the-art controller-free and controller-based multi-object selection methods,  $MOA_s$  significantly reduces task load in the initial selection step of the general multi-object arrangement task.

Table 6: Statistical results of scores (mean value  $\pm$  standard deviation) in SUS under different conditions in user study 1.

QID	Mean $\pm$ SD SUS scores			
	$MOA_s$	<i>Bubble</i>	<i>VVIR</i>	<i>Cone</i>
Q1	$3.7 \pm 0.9$	$3.2 \pm 1.0$	$3.3 \pm 0.7$	$3.3 \pm 0.7$
Q2	$1.9 \pm 0.7$	$2.4 \pm 0.6$	$2.2 \pm 0.7$	$2.4 \pm 0.6$
Q3	$3.3 \pm 1.0$	$3.3 \pm 0.9$	$3.4 \pm 0.9$	$2.9 \pm 0.3$
Q4	$2.2 \pm 0.7$	$2.7 \pm 0.7$	$2.3 \pm 0.7$	$3.0 \pm 0.4$
Q5	$3.7 \pm 0.8$	$3.3 \pm 0.8$	$3.5 \pm 0.7$	$3.0 \pm 0.5$
Q6	$1.1 \pm 0.3$	$1.4 \pm 0.6$	$1.6 \pm 0.6$	$1.7 \pm 0.5$
Q7	$4.4 \pm 0.7$	$3.6 \pm 0.9$	$3.5 \pm 0.6$	$3.2 \pm 0.8$
Q8	$1.1 \pm 0.3$	$1.3 \pm 0.4$	$1.2 \pm 0.4$	$2.4 \pm 0.7$
Q9	$4.2 \pm 0.8$	$3.1 \pm 0.8$	$3.3 \pm 0.7$	$3.0 \pm 1.0$
Q10	$1.0 \pm 0.1$	$1.3 \pm 0.7$	$1.1 \pm 0.5$	$2.6 \pm 0.5$
TOTAL	$79.2 \pm 5.7$	$68.8 \pm 6.5$	$71.6 \pm 5.2$	$57.8 \pm 5.0$

Table 7: Post-hoc analysis of between  $MOA_s$  and other conditions for the SUS total score in user study 1 using Bonferroni.

metric	comparison	mean dif.	std. dif.	p-value
SUS	$MOA_s$	<i>Bubble</i>	10.5	0.7
		<i>VVIR</i>	7.8	0.6
		<i>Cone</i>	12.2	0.1

**Convenience.** In terms of convenience, Table 6 details the SUS statistical results under different method conditions. The effect test across the four conditions for SUS yields ( $F_{3,45} = 16.20$ ,  $p = 7.92 \times 10^{-8}$ ,  $\eta_p^2 = 0.45$ ), indicating significant differences in convenience among the conditions. Compared to other method conditions,  $MOA_s$  achieves a higher SUS total score. Participant feedback demonstrates that  $MOA_s$  effectively presents target objects on the panel for participants to select in the complex scene with high density and occlusion. This instills a strong sense of confidence in participants, leading them to perceive the system not only as easy to use but also as enabling them to efficiently complete a large number of target object selection tasks in complex scenes, resulting in highly positive SUS total scores. Table 7 presents the post-hoc statistical results comparing  $MOA_s$  with the other three conditions for the SUS total score. The p-values indicate that  $MOA_s$  achieves a significantly SUS total score than all other methods. Therefore, we conclude **Conclusion 3**: Compared with all state-of-the-art controller-free and controller-based multi-object selection methods,  $MOA_s$  significantly improves convenience in the initial selection step of the general multi-object arrangement task. Thus, based on **Conclusion 1**, **Conclusion 2**, and **Conclusion 3**, **H3** is supported.

### 3 USER STUDY 2: LATER MANIPULATION EVALUATION

In this section, we conduct user study 2 to further evaluate the task performance, task load, and convenience of MOA's later manipulation step ( $MOA_m$ ) in the multi-object arrangement task, and to compare

$MOA_m$  with state-of-the-art controller-free and controller-based later manipulation methods. We formulate the hypothesis for user study 2 as follows:

**H4.** Compared to state-of-the-art later manipulation methods,  $MOA_m$  significantly improves task performance, reduces task load, and enhances convenience in the later manipulation step of the general multi-object arrangement task.

### 3.1 User Study Design

**Participants and Apparatus.** The same 16 participants from user study 1 are also recruited for user study 2, and the system setup remains consistent between the two user studies.

**Condition.** To comprehensively demonstrate the effectiveness of the proposed  $MOA_m$ , we compare it not only with an existing controller-free method but also with a state-of-the-art controller-based later manipulation method. We use the intuitive Object Proxy method as the controller-free comparison, and VVIR as the controller-based comparison. Thus, the method conditions in user study 2 include  $MOA_m$ , Object Proxy, and VVIR, as shown in Fig. 6.

**Task and Procedure.** The task requires participants to manipulate all target objects to designated target positions in *general scene* using each of the method conditions. Before the task begins, participants spend 1.5 minutes practicing with  $MOA_m$ , Object Proxy, and VVIR to manipulate three selected target objects to their corresponding target positions in the *general scene*. To ensure fair comparisons, the initial object positions for all conditions are identical to those used in previous user studies. Each participant completes 3 trials. The order of these three conditions is counterbalanced across participants using all six possible permutations ( $3! = 6$  orders). Participants are systematically assigned to one of these sequences to mitigate order effects. After each trial, participants complete the NASA-TLX and SUS questionnaires. The entire set of trials takes approximately 25 minutes per participant. A total of 16 (participants)  $\times$  3 (method conditions) = 48 trials are collected.

**Metrics.** We use the objective metric *manipulation time cost* to quantify task performance in the later manipulation step of the multi-object arrangement. The definition of *manipulation time cost* is provided in Section 1. As in user study 1, we employ the standard NASA-TLX questionnaire and SUS to evaluate task load and convenience. Details on the NASA-TLX questionnaire and SUS can be found in Section 2.1.

### 3.2 Results and Discussion

We first assess the normality of the data using Shapiro-Wilk tests and Q-Q plots. For non-normally distributed data, we apply the ART to facilitate transformations. Subsequently, we conduct ANOVA analyses for all comparisons and report effect sizes where applicable. We also perform Bonferroni post-hoc analyses to evaluate individual differences between  $MOA_m$  and the other conditions (Object Proxy, VVIR).

#### Task

In terms of task performance, Fig. 5 visualizes the *manipulation time cost* comparisons in the later manipulation step of the multi-object arrangement task in the *general scene* under three method conditions. The effect test for three conditions in *manipulation time cost* yields ( $F_{2,30} = 167.25$ ,  $p = 1.46 \times 10^{-21}$ ,  $\eta_p^2 = 0.88$ ), indicating significant differences among the conditions

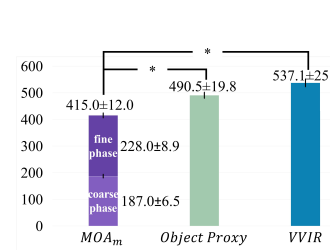


Fig. 5: Mean and standard deviation of *manipulation time cost* in later manipulation using  $MOA_m$ , Object Proxy, and VVIR.

in *manipulation time cost*. Thanks to  $MOA_m$ 's ability to provide corresponding coarse and fine manipulation modes based on different manipulation contexts, participants can quickly manipulate target objects close to the desired target position using the coarse manipulation phase, while the fine manipulation phase allows precise positioning of the object from near the target location to the final target position.

Although fine phase involves less operational distances and angles, its requirement for precision leads to significant time expenditure. Fig. 5 shows that fine manipulation accounts for 80% of the total *manipulation time cost*. However, relying solely on the fine phase makes it difficult to quickly manipulate the object to the vicinity of the target location. Dividing later manipulation into coarse and fine modes is necessary. According to participants' feedback, the two-phase manipulation mode of  $MOA_m$  makes the manipulation process more flexible and efficient, with each mode enabling the realization of specific goals based on the participants' intentions.

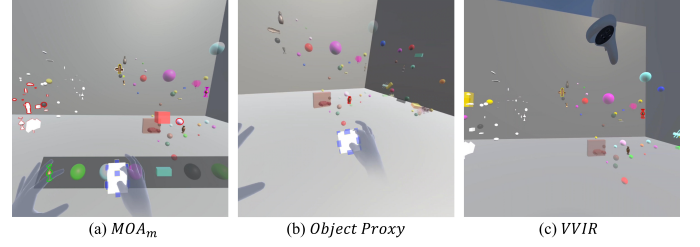


Fig. 6: Visualization of performing later manipulation in *general scene* by using (a) the proposed  $MOA_m$ , (b) Object Proxy, and (c) VVIR.

Table 8: Post-hoc analysis of between  $MOA_m$  and other conditions for the task performance metric in user study 2 using Bonferroni.

metric	comparison	mean dif.	std. dif.	p-value
<i>manipulation time cost</i>	$MOA_m$	-101.3	7.1	$9.6 \times 10^{-18}$
	Object Proxy	-122.1	7.1	$8.0 \times 10^{-21}$

The post-hoc statistical results in Table 8 show that  $MOA_m$  achieves a significant improvement in *manipulation time cost* compared to state-of-the-art method conditions. Therefore, we establish **Conclusion 4**:  $MOA_m$  significantly improves task performance compared to state-of-the-art controller-free and controller-based methods in the later manipulation step of the general multi-object arrangement task.

Table 9: Mean  $\pm$  SD scores of each question in NASA-TLX questionnaire under different conditions in user study 2.

QID	Mean $\pm$ SD NASA-TLX scores		
	$MOA_m$	Object Proxy	VVIR
Q1	27.8 $\pm$ 5.2	30.6 $\pm$ 5.1	31.3 $\pm$ 5.9
Q2	60.0 $\pm$ 8.9	70.0 $\pm$ 8.0	74.4 $\pm$ 9.6
Q3	65.6 $\pm$ 6.0	68.8 $\pm$ 9.2	80.0 $\pm$ 8.6
Q4	30.3 $\pm$ 5.3	33.1 $\pm$ 4.0	57.2 $\pm$ 8.4
Q5	45.6 $\pm$ 4.4	50.3 $\pm$ 8.1	49.4 $\pm$ 8.9
Q6	34.4 $\pm$ 6.8	40.6 $\pm$ 4.4	46.9 $\pm$ 6.4
TOTAL	44.0 $\pm$ 3.3	48.9 $\pm$ 3.4	56.5 $\pm$ 4.0

**Task Load.** Regarding task load, Table 9 presents the detailed NASA-TLX questionnaire results from user study 2. The effect test for three conditions on the NASA-TLX total score yields ( $F_{2,30} = 48.71$ ,  $p = 5.52 \times 10^{-12}$ ,  $\eta_p^2 = 0.68$ ), indicating significant differences among conditions in task load.

Table 10 shows the post-hoc statistical results comparing  $MOA_m$  with the other two conditions for the NASA-TLX score. According to participants' feedback, compared with Object Proxy that requires directly manipulating a large number of target objects,  $MOA_m$  can efficiently manipulate target objects to the vicinity of the corresponding target positions, benefiting from the built-in auxiliary structure. This leaves the precise tuning of complex multi-object manipulation to a more sensitive fine phase of  $MOA_m$ , significantly reducing the physical and cognitive burden on participants. Consequently,  $MOA_m$

Table 10: Post-hoc analysis of between  $MOA_m$  and other conditions for the NASA-TLX total score in user study 2 using Bonferroni.

metric	comparison	mean dif.	std. dif.	p-value
Q1	<i>Object Proxy</i>	-2.8	1.9	$4.5 \times 10^{-1}$
	<i>VVIR</i>	-3.5		$2.4 \times 10^{-1}$
Q2	<i>Object Proxy</i>	-10.0	3.1	$8.0 \times 10^{-4}$
	<i>VVIR</i>	-14.4		$1.2 \times 10^{-4}$
Q3	<i>Object Proxy</i>	-3.2	2.8	$8.4 \times 10^{-1}$
	<i>VVIR</i>	-14.4		$2.3 \times 10^{-5}$
Q4	<i>Object Proxy</i>	-2.8	2.2	$6.1 \times 10^{-1}$
	<i>VVIR</i>	-26.9		$1.6 \times 10^{-15}$
Q5	<i>Object Proxy</i>	-4.7	2.6	$2.4 \times 10^{-1}$
	<i>VVIR</i>	-3.8		$4.8 \times 10^{-1}$
Q6	<i>Object Proxy</i>	-6.3	2.1	$1.4 \times 10^{-2}$
	<i>VVIR</i>	-12.5		$1.0 \times 10^{-6}$
TOTAL	<i>Object Proxy</i>	-4.9	1.3	$1.0 \times 10^{-3}$
	<i>VVIR</i>	-12.5		$2.9 \times 10^{-12}$

scores better than *Object Proxy* on all six dimensions (Q1-Q6) of the NASA-TLX, especially in Q2 (Physical Demands) and Q6 (Frustration), achieving significant advantages of 14.3% and 15.3%, respectively.

*VVIR* integrates a single-step operation mode that forces participants to repeat the entire "aim, move, and place" cycle for each target object when dealing with a large number of target objects. This high frequency of repetitive labor not only leads to participant fatigue but also reduces manipulation accuracy, ultimately making participants feel that they cannot control the entire interaction process.  $MOA_m$ 's two-stage design effectively decouples the complex multi-object manipulation task into coarse and fine phases. First, participants can use guiding structures to quickly and batch manipulate multiple target objects to the vicinity of their respective target locations. Subsequently, they can focus on subsequent fine-grained adjustments. This strategy improves the efficiency and smoothness of the later manipulation task. Therefore,  $MOA_m$  shows improvement over *VVIR* in all question items of NASA-TLX, particularly in Physical Demands (Q2), Temporal Demands (Q3), Own Performance (Q4), and Frustrations (Q6), with gains of 19.4%, 18.0%, 47.0%, and 26.7%, respectively. The *p*-values indicate that  $MOA_m$  achieves significantly better NASA-TLX scores than *Object Proxy* and *VVIR*. Therefore, we obtain **Conclusion 5**: Compared to state-of-the-art controller-free and controller-based methods,  $MOA_m$  significantly reduces task load in the later manipulation step of the general multi-object arrangement task.

**Convenience.** In terms of convenience, Table 11 presents detailed SUS statistical results. The effect test for three conditions on SUS scores yields ( $F_{2,30} = 14.14$ ,  $p = 1.72 \times 10^{-5}$ ,  $\eta_p^2 = 0.39$ ), indicating significant differences among conditions in convenience.

According to participant feedback,  $MOA_m$  facilitates the later manipulation step through a simple pinch-and-release gesture. Furthermore, guided by the auxiliary structure,  $MOA_m$  enables participants to precisely manipulate multiple objects to their designated target positions. Participants perceive  $MOA_m$  is more effective than *Object Proxy* and *VVIR* in multi-object later manipulation tasks. As a result,  $MOA_m$  outperforms the other two method conditions in the SUS total score. Table 12 shows the post-hoc statistical results comparing  $MOA_m$  with the other two conditions for the SUS total score. The *p*-values indi-

cate that  $MOA_m$  achieves significantly higher SUS scores than both *Object Proxy* and *VVIR*. Therefore, we establish **Conclusion 6**: Compared with state-of-the-art controller-free and controller-based methods,  $MOA_m$  significantly improves convenience in the later manipulation step of the general multi-object arrangement task. Thus, based on **Conclusion 4**, **Conclusion 5**, and **Conclusion 6**, the results support **H4**.

Table 11: Mean  $\pm$  SD scores of each question in SUS under different conditions in user study 2.

QID	Mean $\pm$ SD SUS scores		
	$MOA_m$	<i>Object Proxy</i>	<i>VVIR</i>
Q1	$3.9 \pm 0.6$	$3.4 \pm 1.0$	$3.4 \pm 0.8$
Q2	$1.8 \pm 0.7$	$1.9 \pm 0.57$	$2.2 \pm 0.7$
Q3	$3.4 \pm 0.9$	$3.3 \pm 0.8$	$3.3 \pm 0.9$
Q4	$1.8 \pm 0.6$	$2.3 \pm 0.7$	$2.9 \pm 0.9$
Q5	$3.8 \pm 0.7$	$3.6 \pm 0.5$	$3.5 \pm 0.63$
Q6	$1.1 \pm 0.3$	$1.3 \pm 0.5$	$1.4 \pm 0.5$
Q7	$4.3 \pm 0.7$	$3.8 \pm 0.8$	$3.8 \pm 0.7$
Q8	$1.3 \pm 0.5$	$1.4 \pm 0.6$	$1.6 \pm 0.8$
Q9	$4.3 \pm 0.7$	$3.8 \pm 0.7$	$3.4 \pm 0.6$
Q10	$1.3 \pm 0.6$	$1.3 \pm 0.5$	$1.1 \pm 0.3$
TOTAL	$81.4 \pm 5.2$	$73.9 \pm 6.4$	$70.8 \pm 6.0$

Table 12: Post-hoc analysis of between  $MOA_m$  and other conditions for the SUS total score in user study 2 using Bonferroni.

metric	comparison	mean dif.	std. dif.	p-value
SUS	$MOA_m$	<i>Object Proxy</i>	7.5	$2.0 \times 10^{-3}$
		<i>VVIR</i>	10.8	$1.5 \times 10^{-5}$

## REFERENCES

- [1] M. Maslych, Y. Hmaiti, R. Ghamandi, P. Leber, R. K. Kattoju, J. Belga, and J. J. LaViola, "Toward intuitive acquisition of occluded vr objects through an interactive disocclusion mini-map," in *2023 IEEE Conference Virtual Reality and 3D User Interfaces (VR)*. IEEE, 2023, pp. 460–470. [1](#), [3](#)
- [2] J. Bergström, T.-S. Dalsgaard, J. Alexander, and K. Hornbæk, "How to evaluate object selection and manipulation in vr? guidelines from 20 years of studies," in *proceedings of the 2021 CHI conference on human factors in computing systems*, 2021, pp. 1–20. [1](#), [2](#)
- [3] M. R. T. Grady Andersen, "The ultimate guide to vr user testing-bestpractices and essential tools," 2025. [Online]. Available: <https://moldstud.com/articles/p-the-ultimate-guide-to-vr-user-testing-best-practices-and-essential-tools-1>
- [4] F. Welsford-Ackroyd, A. Chalmers, R. Kuffner dos Anjos, D. Medeiros, H. Kim, and T. Rhee, "Spectator view: Enabling asymmetric interaction between hmd wearers and spectators with a large display," *Proceedings of the ACM on Human-Computer Interaction*, vol. 5, no. ISS, pp. 1–17, 2021. [2](#)
- [5] W. Delamare, M. Daniel, and K. Hasan, "Multifingerbubble: A 3d bubble cursor variation for dense environments," in *CHI Conference on Human Factors in Computing Systems Extended Abstracts*, 2022, pp. 1–6. [2](#)
- [6] Q. Zheng, L. Wang, W. Ke, and S. K. Im, "Vvir-om: Efficient object manipulation in vr with variable virtual interaction region," *International Journal of Human-Computer Interaction*, pp. 1–14, 2023. [3](#)
- [7] S. G. Hart and L. E. Staveland, "Development of nasa-tlx (task load index): Results of empirical and theoretical research," in *Advances in psychology*. Elsevier, 1988, vol. 52, pp. 139–183. [3](#)
- [8] J. Brooke *et al.*, "Sus-a quick and dirty usability scale," *Usability evaluation in industry*, vol. 189, no. 194, pp. 4–7, 1996. [3](#)